Osteoarthritis and Cartilage 31 (2023) 482–492

Osteoarthritis and Cartilage

3D analysis and grading of calcifications from ex vivo human meniscus

I. Hellberg † *, V.-P. Karjalainen †, M.A.J. Finnilä †, E. Jonsson ‡ §, A. Turkiewicz ‡, P. Önnerfjord §, V. Hughes ‡, J. Tjörnstrand ||, M. Englund ‡ [a], S. Saarakkala † ¶ [a]

† *Research Unit of Medical Imaging, Physics and Technology, Faculty of Medicine, University of Oulu, Oulu, Finland*
‡ *Lund University, Faculty of Medicine, Department of Clinical Sciences Lund, Orthopaedics, Clinical Epidemiology Unit, Lund, Sweden*
§ *Lund University, Faculty of Medicine, Department of Clinical Sciences Lund, Rheumatology and Molecular Skeletal Biology, Lund, Sweden*
|| *Lund University, Skane University Hospital, Department of Clinical Sciences Lund, Orthopaedics, Lund, Sweden*
¶ *Department of Diagnostic Radiology, Oulu University Hospital, Oulu, Finland*

ARTICLE INFO

Article history:
Received 27 April 2022
Accepted 31 October 2022

Keywords:
Meniscal calcification
Micro-computed tomography
Volumetric analysis
Calcification grading

SUMMARY

Objective: Meniscal calcifications are associated with the pathogenesis of knee osteoarthritis (OA). We propose a micro-computed tomography (μCT) based 3D analysis of meniscal calcifications *ex vivo*, including a new grading system.
Method: Human medial and lateral menisci were obtained from 10 patients having total knee replacement for medial compartment OA and 10 deceased donors without knee OA (healthy references). The samples were fixed; one subsection was imaged with μCT, and the adjacent tissue was processed for histological evaluation. Calcifications were examined from the reconstructed 3D μCT images, and a new grading system was developed. To validate the grading system, meniscal calcification volumes (CV_M) were quantitatively analyzed and compared between the calcification grades. Furthermore, we estimated the relationship between histopathological degeneration and the calcification severity.
Results: 3D μCT images depict calcifications in every sample, including diminutive calcifications that are not visible in histology. In the new grading system, starting from grade 2, each grade results in a CV_M that is 20.3 times higher (95% CI 13.3–30.5) than in the previous grade. However, there was no apparent difference in CV_M between grades 1 and 2. The calcification grades appear to increase with the increasing histopathological degeneration, although histopathological degeneration is also observed with small calcification grades.
Conclusions: 3D μCT grading of meniscal calcifications is feasible. Interestingly, it seems that there are two patterns of degeneration in the menisci of our sample set: 1) with diminutive calcifications (calcification grades 1–2), and 2) with large to widespread calcifications (calcification grades 3–5).

Introduction

Degenerative changes in the meniscus are prevalent in the general population, and they are related to an increased risk of knee osteoarthritis (OA)[1]. Equal to meniscal degradation, meniscal calcifications are strongly associated with knee OA pathogenesis[2,3]. However, the exact role of meniscal calcifications in the OA disease process is currently not well understood.

To date, there are no effective disease-modifying agents on the market that could slow down OA disease progression or reverse it. Regarding pathological calcifications, an antimineralization agent called phosphocitrate has been shown to inhibit meniscal calcification, and concurrently, arrest OA disease progression in a guinea

* Address correspondence and reprint requests to: I. Hellberg, Research Unit of Medical Imaging, Physics and Technology, Faculty of Medicine, University of Oulu, POB 5000, FI-90014 Oulu, Finland. Tel: 358-404129850.
E-mail addresses: iida.hellberg@oulu.fi (I. Hellberg), ville-pauli.karjalainen@oulu.fi (V.-P. Karjalainen), mikko.finnila@oulu.fi (M.A.J. Finnilä), elin.jonsson@maxiv.lu.se (E. Jonsson), aleksandra.turkiewicz@med.lu.se (A. Turkiewicz), patrik.onnerfjord@med.lu.se (P. Önnerfjord), velocity.hughes@med.lu.se (V. Hughes), jon.tjornstrand@med.lu.se (J. Tjörnstrand), martin.englund@med.lu.se (M. Englund), simo.saarakkala@oulu.fi (S. Saarakkala).
[a] Shared senior authorship.

https://doi.org/10.1016/j.joca.2022.10.016

pig model[4]. Furthermore, other phosphocitrate analogs have also been studied in animal models[5–7]. These results indicate that inhibition of pathological calcifications could be a potential therapeutic target for OA. Therefore, having a better understanding of meniscal calcifications would be beneficial.

There are multiple *in vivo* imaging techniques for visualizing and characterizing intra-articular calcifications, including conventional radiography, ultrasonography, (dual-energy) computed tomography, and magnetic resonance imaging[8–17]. While these techniques are important in the clinical evaluation of joint calcification, their spatial resolution is a limiting factor for the visualization and analysis of diminutive calcification deposits in a research setting. The assessment of thin histological sections yields better resolution in the evaluation of meniscal calcifications[18,19]. In addition, transmission electron microscopy (TEM) and high-resolution digital radiography (DR) have been used to analyze calcium deposits in human meniscus[20,21]. These methods, however, are limited to 2D evaluation. We have previously shown that micro-computed tomography (μCT) allows the visualization and quantitative analysis of meniscal soft tissue microstructures in 3D[22,23]. As a continuation, this study presents a μCT-based analysis of meniscal calcifications.

In this study, the objectives were to introduce a μCT-based 3D analysis of meniscal calcifications *ex vivo*, and to describe the different calcification patterns observed in our human sample set of medial and lateral meniscus posterior horns of reference subjects and end-stage medial compartment knee OA patients. Furthermore, we propose a new semi-quantitative grading system for meniscal calcifications and quantitative analysis of calcification volumes (CV_M).

Method

Tissue sample preparation

This study was approved by the regional ethical review board at Lund University (Dnr 2015/39 and Dnr 2016/865). The same sample set was used as in our previous work, where the sample selection and processing are detailed[22]. In short, human meniscus specimens from the knee tissue biobank MENIX at Skåne University Hospital were used. Both the medial and lateral menisci from the right knee of 10 deceased adult donors with no known diagnosis of knee OA or rheumatoid arthritis were selected. We also selected both the medial and lateral menisci from 10 end-stage medial compartment knee OA patients who had a total knee replacement. Both OA and donor groups include five men and five women. Hereafter, the four groups of menisci: medial and lateral donor menisci, and medial and lateral menisci from medial compartment knee OA patients will be referred to as medial^{ref}, lateral^{ref}, medial^{OA}, and lateral^{OA}, respectively. The samples were fixed in 4% saline-buffered formaldehyde, and a tissue piece was then vertically cut from the posterior horns for μCT imaging and analyses. The tissue adjacent to the μCT piece was subjected to histological sample processing and scoring.

μCT imaging of meniscal calcifications

For this analysis, we used the same hexamethyldisilazane (HMDS)-dried μCT samples as in our previous work[22]. However, to obtain optimal calcification contrast, the samples were imaged again with μCT using optimized acquisition parameters, i.e., by increasing the X-ray energy (by increasing the tube voltage and adding a filter) and exposure time. To minimize sample movement during imaging, the samples were fixed to the sample holders with super glue and dental wax. Image acquisition was conducted with a desktop μCT system (SkyScan 1272, Bruker microCT, Kontich, Belgium) with the following settings: tube voltage 50 kV; tube current 200 μA; Al 0.25 mm filtering; isotropic voxel size (2.0 μm)^3; number of projections 2400; averaging five frames/projection; and exposure time 2100 ms. NRecon software (v1.7.1.6, Bruker microCT) was used for image reconstruction, and beam-hardening and ring-artifact corrections were applied during the reconstruction process. Image rendering was performed with CTVox software (v3.3.0 r1412) provided by the μCT manufacturer.

3D grading system for meniscal calcifications

Calcifications were carefully examined visually from the reconstructed 3D μCT images of each sample from all the four sample groups (medial^{ref}, lateral^{ref}, medial^{OA}, and lateral^{OA}). A 3D grading system was developed by modifying a histology-based calcification grading system by Sun *et al.*[18]. The grading criteria were made as straightforward as possible and are based on the size and the location of the calcifications (Table I, Fig. 1). Unlike in the previous system, our grading system gives smaller grades to the small calcifications inside the meniscus than to larger calcifications on the meniscal borders because we wanted to give more weight to the size of the calcifications. The grades range between 0 and 5: grade 0: no calcifications present; grade 1: one or more small punctate calcifications on the meniscus border or multiple borders (femoral, tibial, inner, outer) only; grade 2: one or more small punctate calcifications inside the meniscus with or without one or more small punctate calcifications on any meniscal border; grade 3: one or more large non-punctate calcification clusters on the meniscus border or multiple borders only; grade 4: one or more large non-punctate calcification clusters inside the meniscus with or without one or more large non-punctate calcification clusters on any meniscal border; grade 5: widespread calcifications on the meniscus border or multiple borders and/or inside the meniscus. Calcifications can be considered widespread if they cover 75% of the femoral or tibial border, or in the case of calcification-free borders, if they affect a major proportion of the deeper layers of the meniscus. The grade is given according to the most severe feature observed in the sample. Representative μCT images and the adjacent Alizarin red-stained histological sections of each grade are shown in Fig. 2. A larger image atlas is presented in the supplementary material (Figs. S1–S5).

Reliability and repeatability analysis of the 3D grading system for meniscal calcifications

To assess the inter-observer reliability, two readers (IH & VPK) performed the grading independently on all 40 μCT image stacks. Furthermore, the two readers repeated the grading (with at least a 3-week time difference between the gradings) to analyze the intra-reader reliability. For the second round of grading, the samples were renamed and set in a new randomized order. From each grading round, a consensus grade was given to each sample based on discussion and mutual agreement between the readers. The consensus grades from the first grading round were used throughout the analysis, figures, and tables of this manuscript, and the second consensus grades were only used in the repeatability analysis of the consensus grading.

Volumetric analysis of meniscal calcifications from μCT images

To further validate the grading system, the volumes of meniscal tissue and meniscal calcifications in each sample were calculated from the μCT images using CT Analyser software (ver. 1.20.3.0+, Bruker microCT). Prior to this analysis, bottom parts of the image stacks containing the outer border of the menisci were visually

Grade	
0	No calcifications
1	One or more small punctate calcifications on the meniscus border or multiple borders only
2	One or more small punctate calcifications inside the meniscus with or without one or more small punctate calcifications on any meniscal border
3	One or more large non-punctate calcification clusters on the meniscus border or multiple borders only
4	One or more large non-punctate calcification clusters inside the meniscus with or without one or more large non-punctate calcification clusters on any meniscal border
5	Widespread calcifications on the meniscus border or multiple borders and/or inside the meniscus

Table I

Osteoarthritis and Cartilage

Grading criteria for meniscus calcifications. The grade is given according to the most severe feature observed in the sample. For example, a grade 3 sample can have small punctate calcifications inside and/or on the border(s) of the meniscus if there is also a large non-punctate calcification cluster or clusters on the meniscus border(s)

inspected and the images containing traces of super glue and/or dental wax were removed to only include the meniscal soft tissue and calcifications in the analysis. The analysis pipeline can be divided into three parts: 1) segmentation of the meniscal tissue (soft tissue and calcifications) from the background i.e., preparing the volume of interest in which the calcifications are analyzed, 2) segmenting the calcifications from the meniscal soft tissue and background, and 3) performing the 3D analysis where the volume of meniscal calcifications (CV_M), volume of meniscal tissue (TV_M), and calcification volume fraction (CV_M/TV_M) are calculated (Fig. 3). A more detailed description of the analysis pipeline is provided in the supplementary material (Table S1).

Histological preparation and analyses

Before sectioning, the fixed specimens were dehydrated with alcohol, cleared with xylene, and embedded in paraffin. Vertical sections (4 and 5 μm thick) were cut adjacent to the μCT piece, perpendicular to the circumferentially oriented collagen bundles. The remaining paraffin block was then melted, and the tissue was reoriented and again embedded in paraffin, followed by cutting of horizontal, 4 μm thick sections, adjacent to the vertical sections. Both vertical and horizontal 4 μm thick sections were stained with hematoxylin and eosin (HE), and Safranin-O–Fast Green (SafO–FG). Furthermore, Alizarin red staining was performed on 5 μm thick vertical sections. The stained histological sections were imaged with a digital pathology slide scanner (Aperio AT2, Leica Biosystems, Wetzlar, Germany) with 40× magnification and 0.25 μm pixel size. HE and SafO–FG-stained sections were used for Pauli's histopathological scoring[24]. In the current work, Pauli scores were used to visualize the relationship between histopathological degeneration and calcification severity assessed by the newly developed μCT-based grading system. Alizarin red-stained sections were used for visual inspection of meniscal calcifications (Fig. 2).

Statistical analyses

The descriptive data of the meniscus calcification grades are provided as scatterplots. To assess the inter- and intra-observer reliability, Cohen's linearly weighted kappa coefficients (κ_w) and their 95% confidence intervals (CIs) were calculated using SPSS (IBM SPSS Statistics Version 27.0, Armonk, NY: IBM Corp). To estimate the association between calcification grades and CV_M, a linear mixed regression model with the log of CV_M as an outcome was used. The independent variables were the calcification grade (included as a continuous variable), an indicator for grade 1 (to account for the flattened association at grade 1), and the log of TV_M (to account for varying meniscus sizes). We included a random intercept to account for the dependence of the two menisci from the same knee. The Kenward-Rogers method was used for estimating degrees of freedom due to our small sample size. Residual diagnostics confirmed adequate model fit. Stata version 17 (StataCorp. 2021. Stata Statistical Software: Release 17. College Station, TX: StataCorp LLC.) was used for statistical analyses.

Results

μCT imaging vs histology of meniscal calcifications

Visual examination of the μCT images revealed calcifications in all samples of all groups (Table II, Table S2). Most frequently, calcifications were located on the meniscal borders; even the most healthy-looking samples had minute calcifications on the meniscal borders in our sample set (Table II, Fig. 2, Figs. S1–S2). In the degenerated samples, fibrillated borders and/or clefts were typical locations for calcifications. Furthermore, calcifications inside the meniscus were also relatively common, although they seemed to be less frequent in the lateral^{ref} group. Calcifications near the proteoglycan rich areas and along the collagen fibers, as well as widespread calcifications, were mainly observed in the OA groups (Table II, Table S2).

Compared to μCT, calcifications were not visualized equally well through histology; smaller calcifications that were observed in the reference sample groups in μCT were not visible in the Alizarin red-stained histological sections (Table II, Table S2). Moreover, even though calcifications were observed in most of the OA samples, they were not always easily distinguishable by histology. The calcifications in histology seemed less prevalent and were usually in fewer different locations than in μCT images (Fig. 2, Figs. S1–S5). Notably, histology samples had a lot of tiny particles that slightly resemble calcifications but are probably tissue fragments trapped between the glasses.

3D grading system for meniscal calcifications

The inter- and intra-observer reliability analyses indicated moderate to almost perfect agreement (Table III)[25]. The reliability of the consensus grading suggested substantial to almost perfect agreement (Table III)[25]. Based on this new 3D grading system, when assessing the differences in calcification grades between the

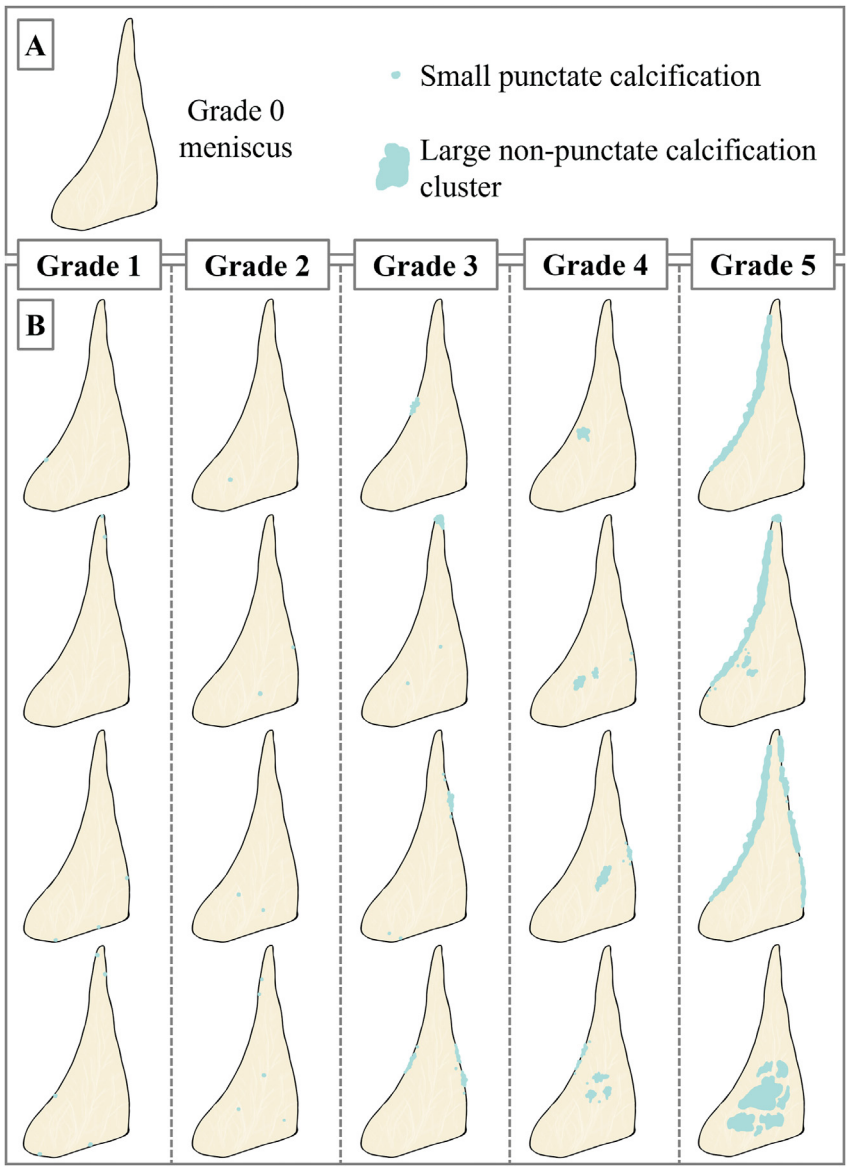

Fig. 1

Osteoarthritis and Cartilage

Calcification grades. A) Left: an example illustration of grade 0 meniscus. Right: example illustrations of a small punctate calcification (observed in grades 1 and 2) and a large non-punctate calcification cluster (observed in grades 3–4). B) Example illustrations of different calcification patterns observed in calcification grades 1–5.

sample groups, medial^{OA} samples appeared to have higher grades than the reference groups (Table S3).

Volumetric analysis of meniscal calcifications from μCT images

When analyzing the differences in CV_M between the different calcification grades, we found that starting from grade 2, each grade results in a CV_M that is 20.3 times higher (95% CI 13.3–30.5) than in the previous grade (Fig. 4). However, there was no apparent difference in CV_M between grade 1 and 2; grade 2 samples had on average 1.64 times larger CV_M (95% CI 0.73–3.67) compared to grade 1 samples.

The relationship between histopathological degeneration and meniscal calcifications

In general, the calcifications increased with increasing histopathological degeneration (Pauli score), and the calcification grades appeared to be the highest in the medial^{OA} group (Fig. 5; study subject-wise presentation in Fig. S6). When focusing specifically on the moderate and severe degeneration grades (Pauli's score 10 and higher), two patterns of degeneration could be identified: one with diminutive calcifications (calcification grades 1–2) and other with large to widespread calcifications (calcification grades 3–5) (Supplementary videos S1 and S2, respectively).

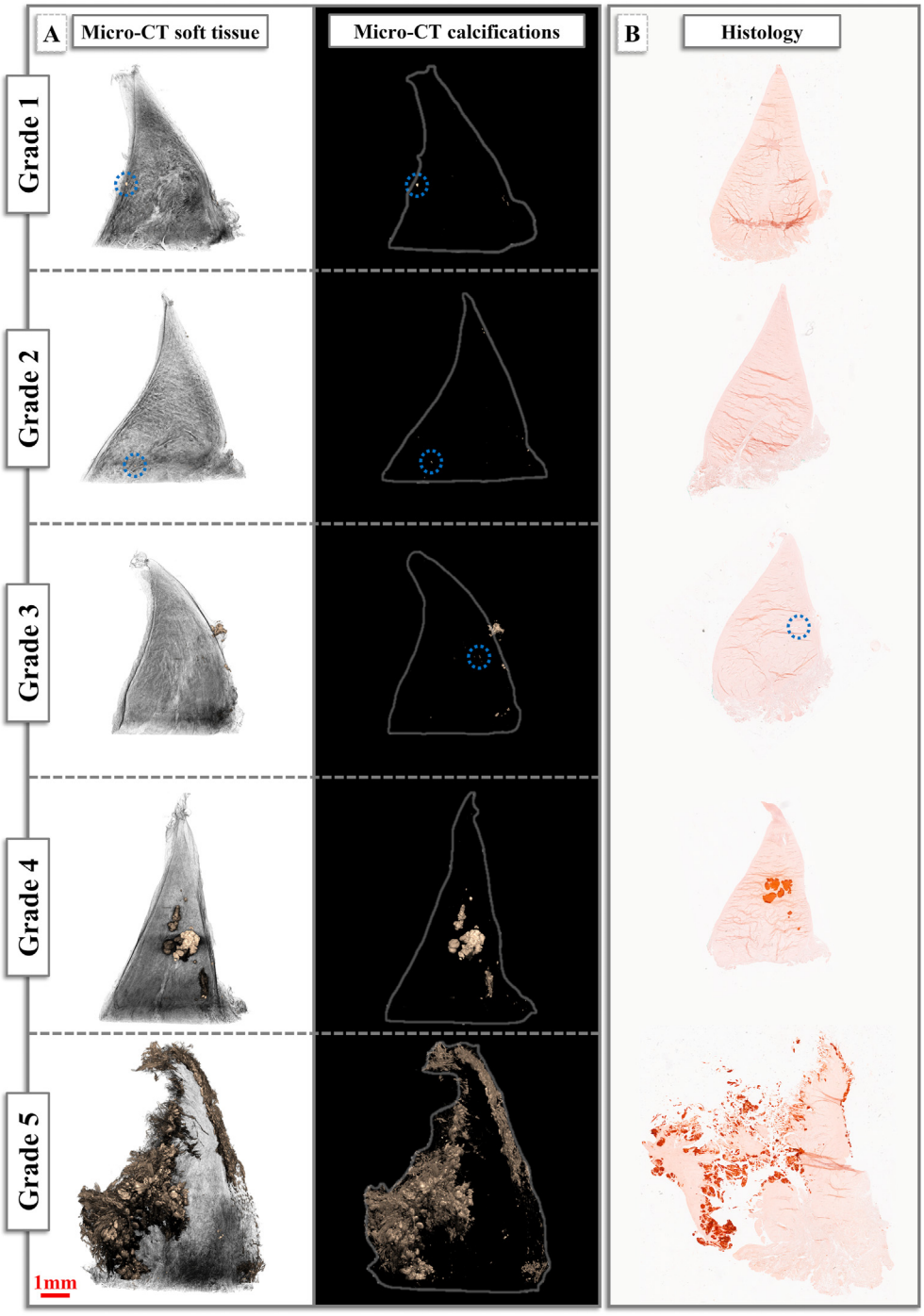

Fig. 2

Osteoarthritis and Cartilage

Meniscus calcification grades. A) Left: representative μCT images of meniscus specimens with the different calcification grades found in our sample set. (Grade 0: no calcifications;) grade 1: one or more small punctate calcifications on the meniscus border or multiple borders (femoral, tibial, inner, outer) only; grade 2: one or more small punctate calcifications inside the meniscus with or without one or more small punctate calcifications on any meniscal border; grade 3: one or more large non-punctate calcification clusters on the meniscus border or multiple borders only; grade 4: one or more large non-punctate calcification clusters inside the meniscus with or without one or more large non-punctate calcification clusters on any meniscal border; grade 5: widespread calcifications on the meniscus borders and/or inside the meniscus. A grade 0 sample is missing because there were at least minor calcifications in all samples. Blue circles mark the location of some of the smaller calcifications. Right: the calcifications from the samples in the left column. The meniscus borders are illustrated with gray lines. B) The Alizarin red-stained histological sections that were taken adjacent to the μCT pieces on the left. With grades 1 and 2, there are no visible calcifications in the histology images although in the same specimens, we can see calcifications in the μCT images.

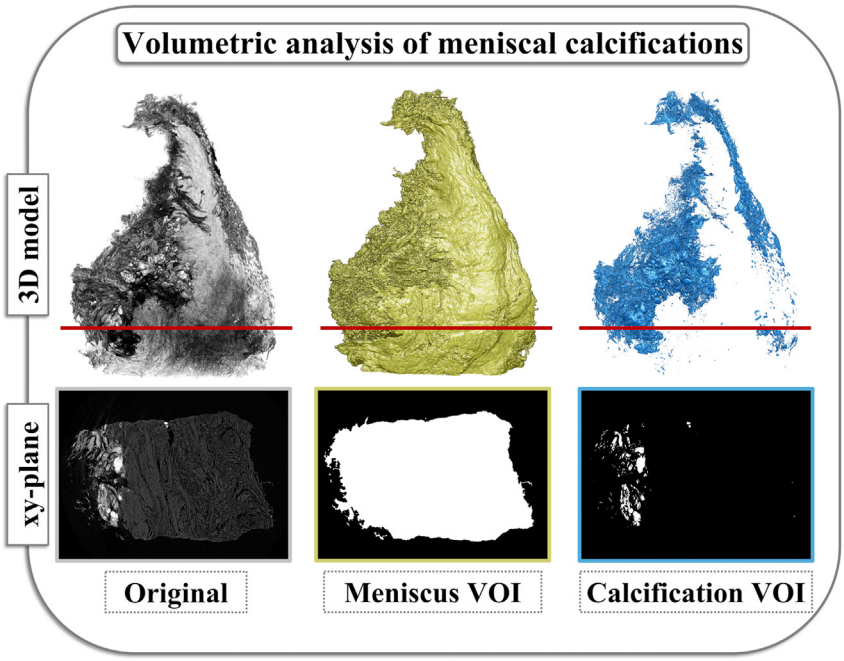

Fig. 3

Osteoarthritis and Cartilage

Volumetric analysis of meniscal calcifications. The top row shows the original μCT, meniscus volume of interest (VOI), and calcification VOI, in a 3D model of a meniscus with calcification grade 5. The transverse lines (in red) show the z-axis location of the xy plane whose 2D images are presented in the bottom row. The pipeline for the 3D analysis of meniscal calcifications can be divided into three parts: first, the meniscal tissue (soft tissue and calcifications) is segmented from the background. In this phase, the VOI in which the calcifications are eventually analyzed is prepared. In the second phase, the calcifications are segmented from the meniscal soft tissue and background. In the final phase, the 3D analysis is performed; the volume of meniscal calcifications (CV_M), volume of meniscal tissue (TV_M), and calcification volume fraction (CV_M/TV_M) are calculated.

Supplementary video related to this article can be found at https://doi.org/10.1016/j.joca.2022.10.016.

Discussion

This study presents a high-resolution μCT-based 3D analysis of meniscal calcifications, including a new calcification grading system. Interestingly, 3D μCT images depicted calcifications in every sample of all groups (Fig. 2, Table II). However, especially the diminutive calcifications were not visible in the adjacent histological sections. Regarding the validation of the developed calcification grading system, the reliability of the consensus gradings suggested substantial to almost perfect agreement (Table III). Furthermore, starting from grade 2, each grade

	Calcification locations	Medial^{OA}	Lateral^{OA}	Medial^{ref}	Lateral^{ref}	Total
μCT	On the meniscus border(s)	10	10	10	10	40 (100%)
	Near the fibrillated edges	9	9	7	5	30 (75%)
	Inside the meniscus	9	8	8	6	31 (78%)
	Near the proteoglycan rich areas*	8	5	4	1	18 (45%)
	Along the collagen fibers	4	3	0	0	7 (18%)
	Widespread	3	0	0	0	3 (8%)
Histology	Visible calcifications in Alizarin red-stained histology	9	8	0	0	17 (43%)
	Near the proteoglycan rich areas†	5	4	0	0	9 (23%)

* Calcifications assessed from μCT, and proteoglycan (PG) rich areas from the adjacent Safranin-O–Fast Green-stained histological sections.
† Calcifications assessed from Alizarin red-stained histological sections, and PG rich areas from the adjacent Safranin-O–Fast Green-stained histological sections.

Table II

Osteoarthritis and Cartilage

Calcification patterns observed in the sample groups ($n = 10$ in each group)

Comparison	κ_w (95% CI)
Inter-reader reliability, medial samples, first reading	0.75 (0.60, 0.89)
Inter-reader reliability, lateral samples, first reading	0.66 (0.45, 0.86)
Inter-reader reliability, medial samples, second reading	0.81 (0.67, 0.95)
Inter-reader reliability, lateral samples, second reading	0.74 (0.53, 0.95)
Intra-reader reliability, reader 1, medial samples	0.89 (0.78, 1.00)
Intra-reader reliability, reader 1, lateral samples	0.71 (0.50, 0.93)
Intra-reader reliability, reader 2, medial samples	0.83 (0.73, 0.94)
Intra-reader reliability, reader 2, lateral samples	0.56 (0.35, 0.76)
Reliability of the consensus grades, medial samples	1.00 (1.00, 1.00)
Reliability of the consensus grades, lateral samples	0.86 (0.71, 1.00)

Table III Osteoarthritis and Cartilage

Reliability results from the μCT calcification grading

resulted in a CV_M that is 20 times higher than in the previous grade, although no apparent difference in CV_M between grade 1 and 2 was found (Fig. 4). Finally, the calcification severity seemed to increase with increasing histopathological degeneration (Fig. 5).

In the visual examination of the μCT images, we found calcification in all samples; even the most healthy-looking samples in the OA-free groups had diminutive calcifications in this sample set, usually on the meniscal borders. However, the calcifications in the OA groups were generally larger and often found in several different locations. Similar observations were made in a previous DR study where meniscal calcifications were observed in all study subjects, with degenerated menisci having more calcifications than healthy ones[21]. The presence of calcification deposits in healthy joints is also supported by a study where hyaline articular cartilage calcifications were detected in all studied knees[26]. On the contrary, intra-articular calcifications were not detected in all study subjects in some of the previous studies[18,27–29]. This could be explained by insufficient resolution and/or lack of sensitivity of the calcification detection techniques.

Compared to μCT, meniscal calcifications were not visualized equally well in histology. No calcifications were detected in the Alizarin red-stained histological sections in the OA-free groups (medial^{ref} and lateral^{ref}). Similar findings have been made in other histology-based studies[18,24]. Consequently, we believe that μCT is a more sensitive method for the detection of diminutive

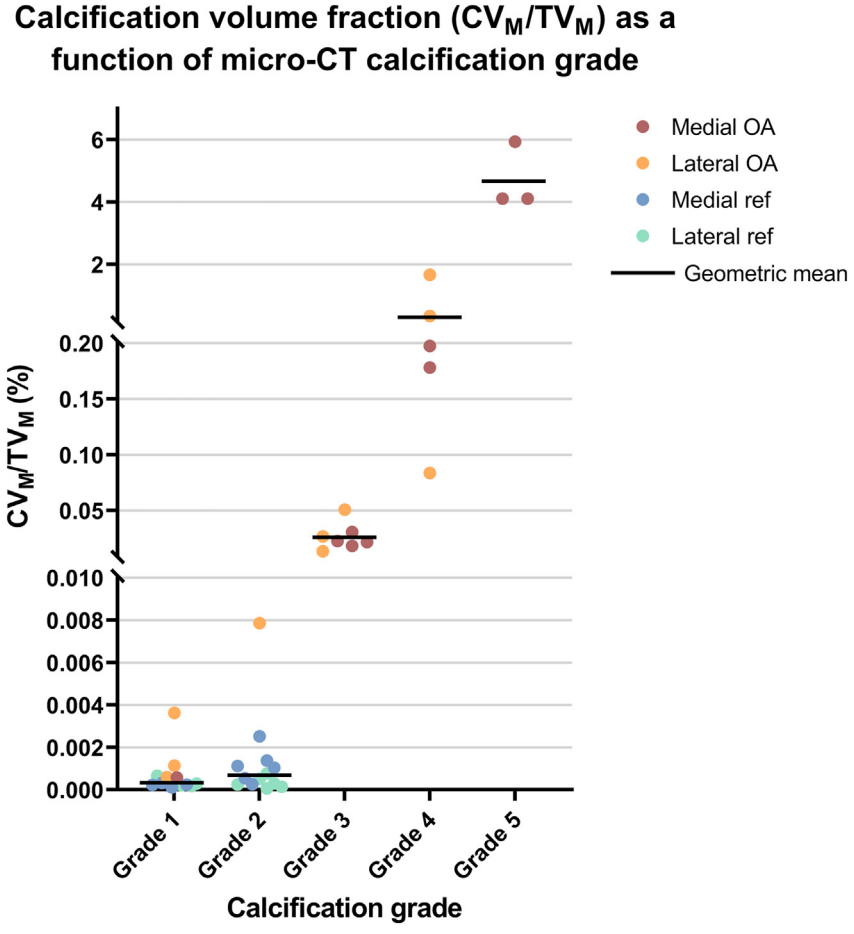

Fig. 4 Osteoarthritis and Cartilage

The relationship between calcification volume fraction (CV_M/TV_M (%)) and the μCT calcification grade.

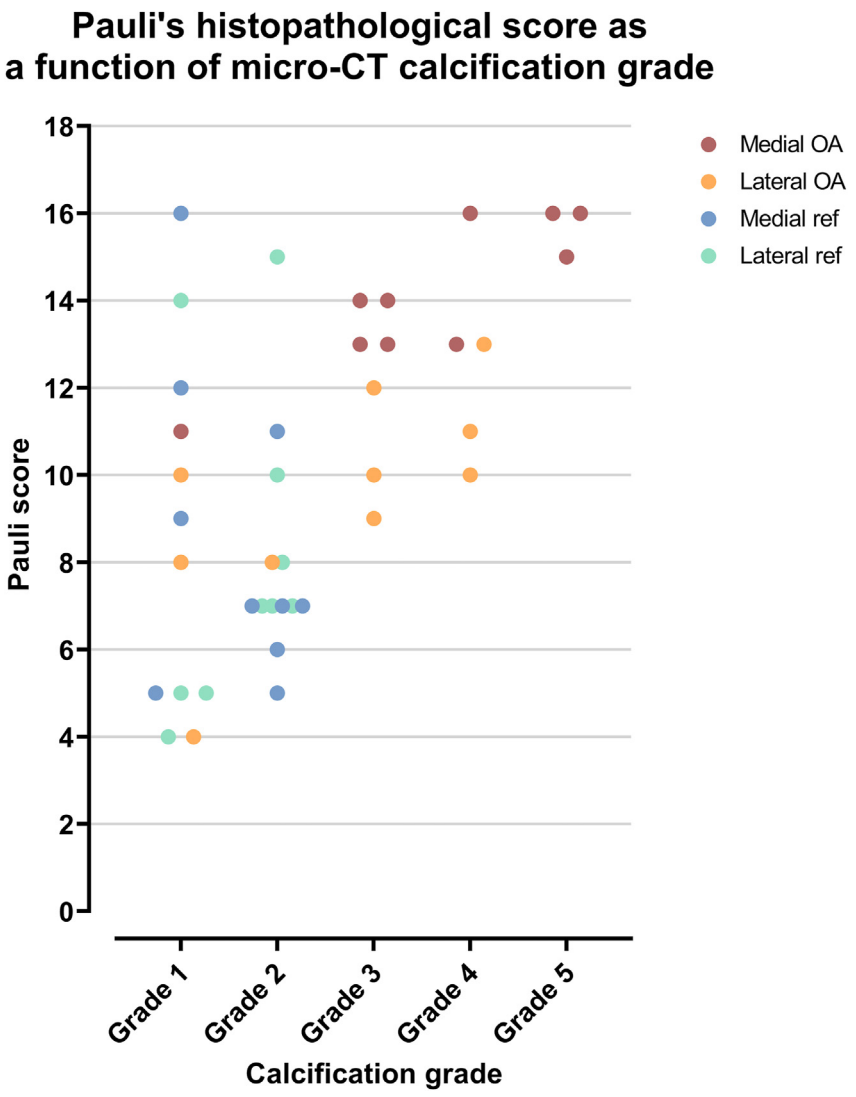

Fig. 5

Osteoarthritis and Cartilage

The relationship between histopathological degeneration (Pauli score) and the μCT calcification grade.

calcifications compared to histology. Supporting this impression, one case showed calcifications with TEM but not with light microscopy in Alizarin red-stained sections in a previous observational study[20]. The lower sensitivity of histology could be explained by small calcifications being torn off from the tissue during the slicing of histological sections or them being dissolved in formalin due to slightly longer preservation time compared to μCT samples, although, our formalin was neutral which should prevent this from happening[30]. Future research is warranted to elucidate how different histological sample processing procedures affect the calcifications. Furthermore, our observations suggest that meniscal calcifications are not spread homogenously in the tissue and may manifest locally, which further limits the calcification detection sensitivity of histological 2D techniques. With μCT, larger volumes can be analyzed with little effort, and hence it is more likely that sparse, small calcifications will be detected.

Calcium pyrophosphate dihydrate (CPP) and basic calcium phosphate (BCP) are the most common calcium crystals found in articular cartilage (in OA)[29,31]. Although their exact role in OA pathogenesis remains to be elucidated, calcium-containing crystals induce inflammation in the joint, and especially BCP crystals appear to contribute to cartilage degradation[32]. Beside OA, the accumulation of CPP crystals is characteristic of CPP crystal deposition (CPPD) disease (also known as chondrocalcinosis or pseudogout). OA is, however, strongly linked to CPPD: according to EULAR recommendations, OA with CPPD is one of the four clinical presentations associated with CPPD[33]. Even though μCT seems to have a good sensitivity in the detection of meniscal calcifications, our methodology cannot differentiate between crystal types in the calcification deposits. Thus, it is uncertain if some of the study subjects in this work were affected by CPPD. To characterize the different crystal types, other modalities such as scanning electron microscopy,

energy dispersive analysis, and Raman spectroscopy could be used[34]. Furthermore, multi-energy photon-counting computed tomography has shown potential in the non-invasive detection and characterization of intra-articular calcifications[35,36]. In our first trials with Raman microspectroscopy, calcifications were detected in the osteoarthritic tissue sections obtained adjacent to the μCT pieces, and only spectra of CPP crystals were identified[37]. In our subsequent study, further analyses will be performed to reliably characterize the crystal types of the calcifications observed in our sample set.

In previous work regarding macroscopic and histopathologic evaluation of human menisci, Pauli *et al.* suggest a separate assessment of calcifications and cell clustering on top of the criteria included in their evaluation system[24]. Several calcification scoring systems exist, for example, CT-based assessment of intra-articular mineralization in human knees, μCT-based scoring of ectopic calcifications in a mouse knee injury model, and radiography-based grading of meniscal mineralization in cats[38–40]. In addition, Sun *et al.* have developed a 5-scale grading system for Alizarin red-stained histological sections from human knee menisci, which is based on the location and size of calcification deposits[18]. This system is perhaps the most compatible with Pauli's histopathological scoring system. Because μCT can depict similar scale features as histology, the new calcification grading system proposed in this study is based on Sun's methodology[18]. The advantage of the 3D μCT approach is that larger specimens can be evaluated without extensive sample processing procedures.

From the inter- and intra-observer reliability analyses, moderate to almost perfect agreement was found in most of the comparisons. The reliability of the consensus gradings suggested substantial to almost perfect agreement[25]. Because consensus grades are used in our analyses, these results can be considered adequate. From the descriptive statistics analyzing the differences in the calcification grades between the sample groups, medial^{OA} samples appeared to have higher grades than the reference groups. The medial^{OA} group is indeed the most affected by OA in our study sample, and therefore was also expected to have the highest calcification grades. This finding is supported by a previous study where the amount of meniscal calcifications was correlated with meniscal degeneration[21]. On the contrary, Mitsyama *et al.* claim that pathological calcification is principally driven by aging rather than OA[26]. The latter work, however, did not include menisci in the study, and the degeneration was assessed solely based on the appearance of the articular surfaces, not using histopathology.

To further validate our new grading system, the CV_M in each sample was calculated from the 3D μCT images, and the association between calcification grades and CV_M was statistically estimated. It was found that starting from grade 2, each grade results in a CV_M that is 20 times higher than in the previous grade. No apparent difference in CV_M between grade 1 and 2 was found. These results indicate that with small punctate calcifications on the meniscus borders and inside the meniscus, the CV_M is similar; however, this suggests that the grading system can differentiate something that the CV_M analysis cannot. To our knowledge, this is the first study to quantitatively evaluate human meniscal calcifications in 3D μCT. Nevertheless, the amount of human meniscal calcifications has previously been quantified in 2D from DR images[21,29]. Comparing these 2D results to our 3D results is, however, unfeasible. Furthermore, volumetric analysis of meniscal calcifications has been performed using CT and μCT images from animal models[41,42], but comparing the results between different species would not be relevant.

When analyzing the association between histopathological degeneration and meniscal calcifications, we found that the calcifications increase with increasing histopathological degeneration, which is supported by a previous cross-sectional DR study[21]. Furthermore, when considering the moderate and severe degeneration grades from Pauli's histopathological scoring system (scores 10 and higher)[24], it seems that two patterns of degeneration occur in the menisci of our sample set: with diminutive calcifications (calcification grades 1–2), and with large to widespread calcifications (calcification grades 3–5). Similar to our findings, Hubert *et al.* also had a wide range of calcification severities in some of their degenerated menisci[21]. Furthermore, while calcifications are associated with OA degeneration[18,24], calcification-free degeneration of meniscus has also previously been reported[43].

This study has some limitations. In general, imaging calcifications with μCT does not require any contrast enhancement. However, because we used the same sample set as in our previous studies[22,23], the samples had been processed with our HMDS protocol to allow the visualization of the soft tissues. It is important to be aware that the HMDS drying might have affected the calcifications, although we found no evidence of this (Fig. S7). Nevertheless, the same protocol was used for each sample and hence the results should be comparable to each other. The second limitation is related to the quantification of CV_M and TV_M. As mentioned in the methods, images containing traces of super glue and/or dental wax in the meniscal outer border area were removed from the analysis to only include the meniscal soft tissue and the calcifications in the analysis. Because of this, parts of meniscal soft tissue, and sometimes calcifications, were left out from the volumetric analysis, which might influence the CV_M and TV_M results. Furthermore, in some samples, the glue traces reached past the meniscal outer border; in such cases the glue traces were manually removed. For future studies, a better method for fixing the samples to the sample holder could be considered. Third, we analyzed only a small piece of each meniscus from posterior horn, which means that our results are primarily generalizable to posterior horn of meniscus. However, since the degenerative changes in the meniscus are most commonly found in the posterior horn and body region[24,44], it was a natural choice. Future studies on the variability of calcifications across meniscus regions are warranted. Fourth, the sample size was relatively small; this is partly explained by the novel analysis method and grading system we were developing and testing. However, the samples represented a wide range of sizes and locations of calcifications. A larger set of samples should be included in future studies to validate our observations. A final limitation is that μCT, like any other imaging modality, has its own intrinsic sources of artifacts. Beam hardening and ring artifacts are the most relevant for this study because they result in a small amount of false positive calcifications in the quantification of CV_M. However, their effect should not be significant because the CV_M is a sum of the volumes of all the separate calcifications (positive and false positive) in each sample. The effect would be more relevant if the separate calcifications were studied and compared individually.

To conclude, we present a high-resolution μCT-based 3D analysis of meniscal calcifications, including a new, validated calcification grading system. 3D μCT grading of meniscal calcifications is feasible: we found that μCT depicts more calcifications compared to conventional 2D histology. Furthermore, when analyzing the relationship between CV_M and the new calcification grade, it was found that starting from grade 2, each grade results in a CV_M that is 20 times higher than in the previous grade. Finally, the calcifications seem to increase with increasing histopathological degeneration. Interestingly, it seems that there are two patterns of degeneration found in menisci of our sample set that may indicate different degenerative processes, or patient responses to meniscal degeneration: 1) with diminutive calcifications (calcification grades 1–2), and 2) with large to widespread calcifications (calcification grades 3–5). Especially for patients belonging to the latter group,

inhibition of pathological calcification might represent a potential therapeutic target for OA management. The proposed grading system could be used to evaluate the efficacy of possible future disease-modifying drugs targeted for calcification inhibition.

Author contributions

Conception and design: IH, MF, SS, and ME.

Provision of study materials and tissue preparation: ME, EJ, VH, PÖ, JT, IH, MF, and SS.

Micro-CT imaging and analysis: IH, VPK, and MF.

Statistical analysis: AT and IH.

Interpretation of results: All coauthors.

Drafting of the article: IH.

Critical revision of the article for important intellectual content: VPK, MF, EJ, AT, PÖ, VH, JT, ME, and SS.

Final approval of the article: All coauthors.

Declaration of competing interest

- AT works as an associate editor (statistics) in Osteoarthritis and Cartilage.
- Other authors (IH, VPK, MF, EJ, PÖ, VH, JT, ME, and SS) report no conflicts of interest.

Role of the funding source

This project has received funding from the Foundation for Research in Rheumatology (FOREUM) (018EnglundPreCl), the European Research Council (ERC) under the European Union's Horizon 2020 research and innovation programme (grant agreement No 771121), The Swedish Research Council, Governmental funding of clinical research within the national health services (ALF), The Swedish Rheumatism Association, Österlund Foundation, and Sigrid Jusélius Foundation. IH has received grants from Finnish Foundation for Technology Promotion (Grant No. 6562), and Instrumentarium Science Foundation (Grant No. 210036).

The funders had no role in study design, data collection and analysis, decision to publish, or preparation of the manuscript.

Acknowledgments

We would like to thank the MENIX clinical staff at Trelleborg Hospital, the Tissue Donor Bank at Skåne University Hospital, and the Department of Forensic Medicine in Lund for their collaboration that enabled sample collection. We would also like to acknowledge Tarja Huhta and Piia Mäkelä, Laboratory Technicians, for preparatory work with the histological samples.

Supplementary data

Supplementary data to this article can be found online at https://doi.org/10.1016/j.joca.2022.10.016.

References

1. Englund M, Roos EM, Lohmander LS. Impact of type of meniscal tear on radiographic and symptomatic knee osteoarthritis: a sixteen-year followup of meniscectomy with matched controls. Arthritis Rheumatol 2003;48(8):2178–87, https://doi.org/10.1002/art.11088.
2. Sun Y, Mauerhan DR. Meniscal calcification, pathogenesis and implications. Curr Opin Rheumatol 2012;24(2), https://journals.lww.com/co-rheumatology/Fulltext/2012/03000/Meniscal_calcification,_pathogenesis_and.6.aspx.
3. McCarthy GM, Cheung HS. Point: hydroxyapatite crystal deposition is intimately involved in the pathogenesis and progression of human osteoarthritis. Curr Rheumatol Rep 2009;11(2):141–7, https://doi.org/10.1007/s11926-009-0020-6.
4. Cheung HS, Sallis JD, Demadis KD, Wierzbicki A. Phosphocitrate blocks calcification-induced articular joint degeneration in a Guinea pig model. Arthritis Rheumatol 2006;54(8):2452–61, https://doi.org/10.1002/art.22017.
5. Sun Y, Haines N, Roberts A, Ruffolo M, Mauerhan DR, Mihalko KL, *et al*. Disease-modifying effects of phosphocitrate and phosphocitrate-β-ethyl ester on partial meniscectomy-induced osteoarthritis. BMC Musculoskelet Disord 2015;16(1):270, https://doi.org/10.1186/s12891-015-0724-x.
6. Sun Y, Roberts A, Mauerhan DR, Cox M, Hanley EN. Biological effects and osteoarthritic disease-modifying activity of small molecule CM-01. J Orthop Res 2018;36(1):309–17, https://doi.org/10.1002/jor.23616.
7. Sun Y, Kiraly AJ, Sun AR, Cox M, Mauerhan DR, Hanley EN. Effects of a phosphocitrate analogue on osteophyte, subchondral bone advance, and bone marrow lesions in Hartley Guinea pigs. Bone Jt Res 2018;7(2):157–65, https://doi.org/10.1302/2046-3758.72.BJR-2017-0253.
8. Barskova VG, Kudaeva FM, Bozhieva LA, Smirnov AV, Volkov Av, Nasonov EL. Comparison of three imaging techniques in diagnosis of chondrocalcinosis of the knees in calcium pyrophosphate deposition disease. Rheumatology 2013;52(6):1090–4, https://doi.org/10.1093/rheumatology/kes433.
9. Misra D, Guermazi A, Sieren JP, Lynch J, Torner J, Neogi T, *et al*. CT imaging for evaluation of calcium crystal deposition in the knee: initial experience from the Multicenter Osteoarthritis (MOST) study. Osteoarthr Cartil 2015;23(2):244–8, https://doi.org/10.1016/j.joca.2014.10.009.
10. Budzik JF, Marzin C, Legrand J, Norberciak L, Becce F, Pascart T. Can dual-energy computed tomography be used to identify early calcium crystal deposition in the knees of patients with calcium pyrophosphate deposition? Arthritis Rheumatol 2021;73(4):687–92, https://doi.org/10.1002/art.41569.
11. Omoumi P, Bae WC, Du J, Diaz E, Statum S, Bydder GM, *et al*. Meniscal calcifications: morphologic and quantitative evaluation by using 2D inversion-recovery ultrashort echo time and 3D ultrashort echo time 3.0-T MR imaging techniques—feasibility study. Radiology 2012;264(1):260–8, https://doi.org/10.1148/radiol.12111439.
12. Tedeschi SK, Becce F, Pascart T, Guermazi A, Budzik JF, Dalbeth N, *et al*. Imaging features of calcium pyrophosphate deposition (CPPD) disease: consensus definitions from an international multidisciplinary working group. Arthritis Care Res 2022, https://doi.org/10.1002/acr.24898.
13. Cipolletta E, Filippou G, Scirè CA, di Matteo A, di Battista J, Salaffi F, *et al*. The diagnostic value of conventional radiography and musculoskeletal ultrasonography in calcium pyrophosphate deposition disease: a systematic literature review and meta-analysis. Osteoarthr Cartil 2021;29(5):619–32, https://doi.org/10.1016/j.joca.2021.01.007.
14. Pascart T, Norberciak L, Legrand J, Becce F, Budzik JF. Dual-energy computed tomography in calcium pyrophosphate deposition: initial clinical experience. Osteoarthr Cartil 2019;27(9):1309–14, https://doi.org/10.1016/j.joca.2019.05.007.
15. Pascart T, Falgayrac G, Norberciak L, Lalanne C, Legrand J, Houvenagel E, *et al*. Dual-energy computed-tomography-based discrimination between basic calcium phosphate and calcium pyrophosphate crystal deposition in vivo. Ther Adv Musculoskelet Dis 2020;12. 1759720X20936060. https://doi.org/10.1177/1759720X20936060.

16. Finkenstaedt T, Biswas R, Abeydeera NA, Siriwanarangsun P, Healey R, Statum S, *et al*. Ultrashort time to echo magnetic resonance evaluation of calcium pyrophosphate crystal deposition in human menisci. Investig Radiol 2019;54(6):349–55, https://doi.org/10.1097/RLI.0000000000000547.
17. Germann C, Galley J, Falkowski AL, Fucentese SF, Pfirrmann CWA, Nanz D, *et al*. Ultra-high resolution 3D MRI for chondrocalcinosis detection in the knee-a prospective diagnostic accuracy study comparing 7-tesla and 3-tesla MRI with CT. Eur Radiol 2021;31(12):9436–45, https://doi.org/10.1007/s00330-021-08062-x.
18. Sun Y, Mauerhan DR, Honeycutt PR, Kneisl JS, Norton HJ, Zinchenko N, *et al*. Calcium deposition in osteoarthritic meniscus and meniscal cell culture. Arthritis Res Ther 2010;12(2). R56–R56. https://doi.org/10.1186/ar2968.
19. Kiraly AJ, Roberts A, Cox M, Mauerhan D, Hanley E, Sun Y. Comparison of meniscal cell-mediated and chondrocyte-mediated calcification. Open Orthop J 2017;11:225–33, https://doi.org/10.2174/1874325001711010225.
20. Battistelli M, Favero M, Burini D, Trisolino G, Dallari D, de Franceschi L, *et al*. Morphological and ultrastructural analysis of normal, injured and osteoarthritic human knee menisci. Eur J Histochem 2019;63(1), https://doi.org/10.4081/ejh.2019.2998.
21. Hubert J, Beil FT, Rolvien T, Butscheidt S, Hischke S, Püschel K, *et al*. Cartilage calcification is associated with histological degeneration of the knee joint: a highly prevalent, age-independent systemic process. Osteoarthr Cartil 2020;28(10):1351–61, https://doi.org/10.1016/j.joca.2020.04.020.
22. Kestilä I, Folkesson E, Finnilä MA, Turkiewicz A, Önnerfjord P, Hughes V, *et al*. Three-dimensional microstructure of human meniscus posterior horn in health and osteoarthritis. Osteoarthr Cartil 2019;27(12):1790–9, https://doi.org/10.1016/j.joca.2019.07.003.
23. Karjalainen VP, Kestilä I, Finnilä MA, Folkesson E, Turkiewicz A, Önnerfjord P, *et al*. Quantitative three-dimensional collagen orientation analysis of human meniscus posterior horn in health and osteoarthritis using micro-computed tomography. Osteoarthr Cartil 2021;29(5):762–72, https://doi.org/10.1016/j.joca.2021.01.009.
24. Pauli C, Grogan SP, Patil S, Otsuki S, Hasegawa A, Koziol J, *et al*. Macroscopic and histopathologic analysis of human knee menisci in aging and osteoarthritis. Osteoarthr Cartil 2011;19(9):1132–41, https://doi.org/10.1016/j.joca.2011.05.008.
25. Landis JR, Koch GG. The measurement of observer agreement for categorical data. Biometrics 1977;33(1):159–74, https://doi.org/10.2307/2529310.
26. Mitsuyama H, Healey RM, Terkeltaub RA, Coutts RD, Amiel D. Calcification of human articular knee cartilage is primarily an effect of aging rather than osteoarthritis. Osteoarthr Cartil 2007;15(5):559–65, https://doi.org/10.1016/j.joca.2006.10.017.
27. Mitrovic DR, Stankovic A, Iriarte-Borda O, Uzan M, Quintero M, Miravet L, *et al*. The prevalence of chondrocalcinosis in the human knee joint. An autopsy survey. J Rheumatol 1988;15(4):633–41, http://europepmc.org/abstract/MED/3397973.
28. Abreu M, Johnson K, Chung CB, de Lima JE, Trudell D, Terkeltaub R, *et al*. Calcification in calcium pyrophosphate dihydrate (CPPD) crystalline deposits in the knee: anatomic, radiographic, MR imaging, and histologic study in cadavers. Skelet Radiol 2004;33(7):392–8, https://doi.org/10.1007/s00256-004-0767-9.
29. Fuerst M, Bertrand J, Lammers L, Dreier R, Echtermeyer F, Nitschke Y, *et al*. Calcification of articular cartilage in human osteoarthritis. Arthritis Rheumatol 2009;60(9):2694–703, https://doi.org/10.1002/art.24774.
30. Boskey AL, Cohen ML, Bullough PG. Hard tissue biochemistry: a comparison of fresh-frozen and formalin-fixed tissue samples. Calcif Tissue Int 1982;34(1):328–31.
31. Molloy ES, McCarthy GM. Calcium crystal deposition diseases: update on pathogenesis and manifestations. Rheum Dis Clin N Am 2006;32(2):383–400, https://doi.org/10.1016/j.rdc.2006.02.001.
32. Conway R, McCarthy GM. Calcium-containing crystals and osteoarthritis: an unhealthy alliance. Curr Rheumatol Rep 2018;20(3):13, https://doi.org/10.1007/s11926-018-0721-9.
33. Zhang W, Doherty M, Bardin T, Barskova V, Guerne PA, Jansen TL, *et al*. European league against rheumatism recommendations for calcium pyrophosphate deposition. Part I: terminology and diagnosis. Ann Rheum Dis 2011;70(4):563–70, https://doi.org/10.1136/ard.2010.139105.
34. Hawellek T, Hubert J, Hischke S, Krause M, Bertrand J, Schmidt BC, *et al*. Calcification of the acetabular labrum of the hip: prevalence in the general population and relation to hip articular cartilage and fibrocartilage degeneration. Arthritis Res Ther 2018;20(1):104, https://doi.org/10.1186/s13075-018-1595-y.
35. Stamp LK, Anderson NG, Becce F, Rajeswari M, Polson M, Guyen O, *et al*. Clinical utility of multi-energy spectral photon-counting computed tomography in crystal arthritis. Arthritis Rheumatol 2019;71(7):1158–62, https://doi.org/10.1002/art.40848.
36. Bernabei I, Sayous Y, Raja AY, Amma MR, Viry A, Steinmetz S, *et al*. Multi-energy photon-counting computed tomography versus other clinical imaging techniques for the identification of articular calcium crystal deposition. Rheumatology 2021;60(5):2483–5, https://doi.org/10.1093/rheumatology/keab125.
37. das Gupta S, Hellberg I, Karjalainen VP, Nissinen R, Jonsson E, Önnerfjord P, *et al*. Characterization of the calcifications in the posterior horn of human meniscus via Raman microspectroscopy. Osteoarthr Cartil 2022;30:S279–80.
38. Guermazi A, Jarraya M, Lynch JA, Felson DT, Clancy M, Nevitt M, *et al*. Reliability of a new scoring system for intra-articular mineralization of the knee: Boston University Calcium Knee Score (BUCKS). Osteoarthr Cartil 2020;28(6):802–10, https://doi.org/10.1016/j.joca.2020.03.003.
39. Rai MF, Schmidt EJ, Hashimoto S, Cheverud JM, Sandell LJ. Genetic loci that regulate ectopic calcification in response to knee trauma in LG/J by SM/J advanced intercross mice. J Orthop Res 2015;33(10):1412–23, https://doi.org/10.1002/jor.22944.
40. Freire M, Brown J, Robertson ID, Pease AP, Hash J, Hunter S, *et al*. Meniscal mineralization in domestic cats. Vet Surg 2010;39(5):545–52, https://doi.org/10.1111/j.1532-950X.2010.00648.x.
41. Stone AV, Vanderman KS, Willey JS, Long DL, Register TC, Shively CA, *et al*. Osteoarthritic changes in vervet monkey knees correlate with meniscus degradation and increased matrix metalloproteinase and cytokine secretion. Osteoarthr Cartil 2015;23(10):1780–9, https://doi.org/10.1016/j.joca.2015.05.020.
42. Kapadia RD, Badger AM, Levin JM, Swift B, Bhattacharyya A, Dodds RA, *et al*. Meniscal ossification in spontaneous osteoarthritis in the Guinea-pig. Osteoarthr Cartil 2000;8(5):374–7, https://doi.org/10.1053/joca.1999.0312.
43. Noble J, Hamblen DL. The pathology of the degenerate meniscus lesion. J Bone Jt Surg 1975;57(2):180–6.
44. Englund M, Guermazi A, Gale D, Hunter DJ, Aliabadi P, Clancy M, *et al*. Incidental meniscal findings on knee MRI in middle-aged and elderly persons. N Engl J Med 2008;359(11):1108–15, https://doi.org/10.1056/NEJMoa0800777.